Water Splitting | Hot Paper

DOI: 10.1002/ange.201404926

Plasmon-Assisted Water Splitting Using Two Sides of the Same $SrTiO_3$ Single-Crystal Substrate: Conversion of Visible Light to Chemical Energy**

*Yuqing Zhong, Kosei Ueno, Yuko Mori, Xu Shi, Tomoya Oshikiri, Kei Murakoshi, Haruo Inoue, and Hiroaki Misawa**

Abstract: *A plasmon-induced water splitting system that operates under irradiation by visible light was successfully developed; the system is based on the use of both sides of the same strontium titanate ($SrTiO_3$) single-crystal substrate. The water splitting system contains two solution chambers to separate hydrogen (H_2) and oxygen (O_2). To promote water splitting, a chemical bias was applied by regulating the pH values of the chambers. The quantity of H_2 evolved from the surface of platinum, which was used as a reduction co-catalyst, was twice the quantity of O_2 evolved from an Au-nanostructured surface. Thus, the stoichiometric evolution of H_2 and O_2 was clearly demonstrated. The hydrogen-evolution action spectrum closely corresponds to the plasmon resonance spectrum, indicating that the plasmon-induced charge separation at the Au/$SrTiO_3$ interface promotes water oxidation and the subsequent reduction of a proton on the backside of the $SrTiO_3$ substrate. The chemical bias is significantly reduced by plasmonic effects, which indicates the possibility of constructing an artificial photosynthesis system with low energy consumption.*

To solve the global energy problem, the development of a system that converts solar energy to not only electrical but also chemical energy that can be stored for long periods is critical.[1] Honda and Fujishima have developed photoelectric conversion and photoelectrochemical water splitting systems that use a titanium dioxide (TiO_2) photoelectrode irradiated by ultraviolet light.[2] However, only approximately 5% of the solar irradiance observed on the Earth's surface is composed of ultraviolet radiation (< 400 nm), whereas visible light (400–800 nm) and infrared light (> 800 nm) represent 50% and 45%, respectively. Therefore, the extension of light-energy conversion to longer wavelengths, especially to the visible and near-infrared regions, is important.[3] The conversion of visible light can be achieved by several methods, including the use of a Z-Scheme electron transfer process,[4] the use of TiO_2 with the addition of certain dopants,[5] and the use of semiconductor nanoparticles with a bandgap wavelength in the visible wavelength region.[6] To date, semiconductor particles have been used to induce hydrogen and oxygen evolution through the response of such photocatalysts to visible light.[7] One of the disadvantages of the use of semiconductor particles in a photocatalytic water splitting system that requires energy to separate H_2 from O_2 is that H_2 and O_2 are evolved in the same reaction chamber.[8] Recently, the evolution of H_2 and O_2 in different reaction chambers has been studied using photoelectrodes fabricated by sintering semiconductor particles.[9] Except for the Z-Scheme reaction system, such systems do not require cathode irradiation because hydrogen evolution occurs by a dark reaction. Therefore, the optimization of a reaction cell design that can effectively use light for water splitting is expected. In this study, we propose that the simultaneous evolution of H_2 and O_2 can be realized without an electric wire connecting the anode and the cathode and with space conserved for light irradiation on the anode side through the use of two sides of the same semiconductor substrate. In the present study, we describe a plasmon-induced water splitting system that responds to visible light and is based on gold nanoparticles (Au-NPs) loaded onto $SrTiO_3$ single-crystal substrates. We also demonstrate the successful separation of H_2 and O_2 in different chambers using both sides of the same substrate.

A scanning electron microscope image of Au-NPs on a 0.05 wt% niobium-doped strontium titanate (Nb-$SrTiO_3$) single-crystal substrate is shown in Figure 1a. In this study, $SrTiO_3$ was employed for the semiconductor substrate because the conduction band energy is negative as compared to the redox potential of H_2. The average size of the Au-NPs is

[*] Y. Zhong, Prof. K. Ueno, Y. Mori, Dr. X. Shi, Dr. T. Oshikiri, Prof. H. Misawa
Research Institute for Electronic Science
Hokkaido University N21, W10, CRIS Building
Kita-ku, Sapporo 001-0021 (Japan)
E-mail: misawa@es.hokudai.ac.jp
Homepage: http://misawa.es.hokudai.ac.jp/index_en.html
Prof. K. Murakoshi
Graduate School of Science, Hokkaido University
Sapporo 060-0810 (Japan)
Prof. H. Inoue
Center for Artificial Photosynthesis, Tokyo Metropolitan University
1-1 Minami-Ohsawa, Hachiohji, Tokyo 192-0397 (Japan)

[**] The authors acknowledge Prof. Tsukasa Torimoto at Nagoya University for productive discussions about the mechanism of the water-splitting device. This study was supported by funding from the Ministry of Education, Culture, Sports, Science, and Technology of Japan: KAKENHI Grant-in-Aid for Scientific Research (grant number 23225006) and the Innovative Areas "Artificial Photosynthesis (AnApple)" (grant number 25107501) grant from the Japan Society for the Promotion of Science (JSPS), the Nanotechnology Platform (Hokkaido University), and the Low-Carbon Research Network of Japan. This study was also supported by the China Scholarship Council (CSC).

Supporting information for this article is available on the WWW under http://dx.doi.org/10.1002/anie.201404926.

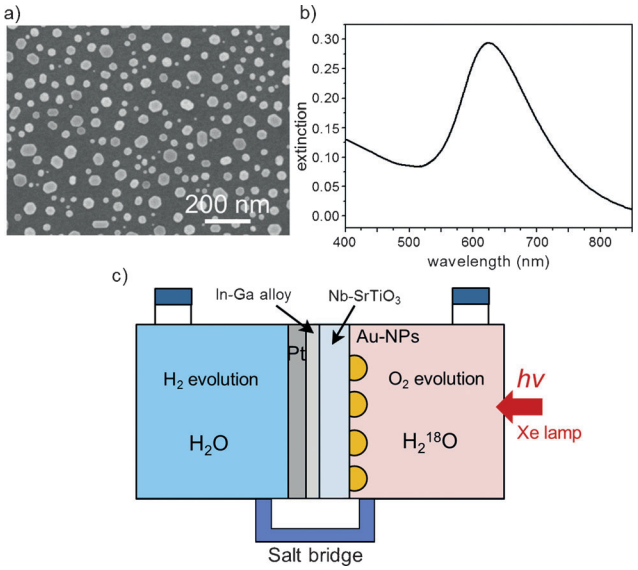

Figure 1. a) Scanning electron microscope image of Au-NPs on Nb-$SrTiO_3$ prepared by anneal method (the scale bar is 200 nm). b) Extinction spectrum of the Au-NPs on Nb-$SrTiO_3$. c) A schematic illustration of the water splitting device using the Au-NP-loaded Nb-$SrTiO_3$ photoelectrode.

52 nm, and the standard deviation of the structural size is estimated to be 10 nm. Figure 1b shows the extinction spectrum of the Au-NPs on the Nb-$SrTiO_3$ substrate. A localized surface plasmon resonance (LSPR) band at 630 nm is clearly visible. A schematic illustration of the water splitting system based on the Au-NP-loaded Nb-$SrTiO_3$ substrate is shown in Figure 1c. In the front chamber, O_2 evolution is expected to follow the plasmon-induced charge separation and the subsequent water oxidation. The evolution of H_2 is expected in the back chamber because of the reduction of protons by photogenerated electrons injected into the conduction band of Nb-$SrTiO_3$ at the Pt surface, which was used as a reduction co-catalyst.[10] To maintain the charge balance between these compartments, a conventional salt bridge containing 2 wt% agar was employed.

Figure 2a depicts the irradiation time dependence of H_2 and O_2 evolution in the backside and frontside chambers, respectively. Experimental details about the quantitative determination of H_2 and O_2 evolution are given in the Supporting Information. The pH value was adjusted to 1 on the H_2-evolution side, whereas the pH value on the O_2-evolution side was adjusted to 13. A xenon light spectrally filtered over the wavelength range of 450 to 850 nm was used to irradiate the Au-NPs and induce LSPR. Under the irradiation conditions, the evolution of H_2 and O_2 increased linearly with increasing irradiation time. As for the time dependence of H_2 and O_2 evolutions, linearity was maintained in the irradiation time, and it was not a quantity of evolution to the extent that pH changes. Actually, we confirmed that the pH value did not change before or after the irradiation. In a separate experiment, we confirmed that neither H_2 nor O_2 was evolved from a Nb-$SrTiO_3$ substrate without Au-NPs under the same irradiation conditions. No production of H_2 or O_2 was observed in the absence of irradiation for an extended period (6 h), even when the Au-NP-loaded Nb-$SrTiO_3$ substrate was used. Figure 2a shows that the quantity of H_2 evolved from the surface of Pt, which was used as a reduction co-catalyst, is twice the quantity of O_2 evolved from the Au nanostructured surface. Therefore, the stoichiometric evolution of H_2 and O_2 was clearly demonstrated in the water splitting system based on the Au-NP-loaded Nb-$SrTiO_3$ single-crystal substrate.

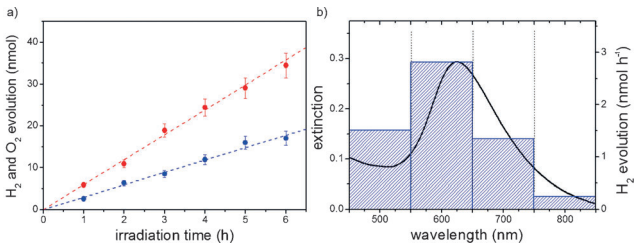

Figure 2. a) An irradiation time dependence of H_2 (red circle) and O_2 (blue circle) evolution obtained in back and front side chamber, respectively. b) The action spectrum of H_2 evolution with several wavelength regions using a histogram. The solid line indicates the LSPR band already shown in Figure 1b.

The histogram in Figure 2b shows the action spectrum of H_2 evolution. The pH conditions used were a pH of 1 for the H_2-evolution side and a pH of 13 for the O_2-evolution side. In the 600 ± 50 nm, 700 ± 50 nm, and 800 ± 50 nm wavelength regions, the evolution efficiency (mol per hour) of H_2 is in approximate agreement with the LSPR band indicated by the solid line in Figure 2b, whereas the evolution efficiency of H_2 in the 500 ± 50 nm wavelength region is higher than that indicated by the spectrum of the Au-NPs on the Nb-$SrTiO_3$. This result indicates that H_2 and O_2 evolution was induced not only by LSPR excitation but also by the direct excitation of the interband transition from the d-bands to the sp-conduction band of gold in the 500 ± 50 nm wavelength region. Thus, the H_2-evolution efficiency in the shorter-wavelength region is higher than that in the longer-wavelength region. Notably, the water splitting is closely related to the LSPR excitation because the evolution efficiency of H_2 is strongly dependent on the LSPR band.

To further understand this system in detail, we performed a pH-dependence experiment to investigate the effect of the chemical bias on the water splitting. In the experiment, a xenon light spectrally filtered over the wavelength range of 550 nm to 650 nm with an intensity of 0.32 $W cm^{-2}$ was used for the LSPR excitation. Figure 3a indicates the representative irradiation time dependence of H_2 and O_2 evolution at the pH combination of 1 and 13. The evolution of both H_2 and O_2 increases linearly with increasing irradiation time, and the quantity of H_2 evolved is twice that of O_2 evolved, which is analogous to the results in Figure 2a. Figure 3b shows the pH dependence of the H_2 and O_2 evolution efficiency. The pH value on the O_2-evolution side was fixed at 13, as indicated by the blue background in Figure 3b, which is the condition that preferentially induces water oxidation. The evolution efficiency of H_2 is twice that of O_2 at the observed pH value. However, the evolution efficiency of both H_2 and O_2 gradually decreased with increasing pH value on the H_2-

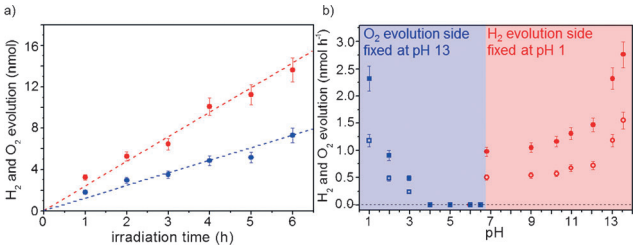

Figure 3. a) An irradiation time dependence of H_2 (red circle) and O_2 (blue circle) evolution at the pH combination of 1 and 13 under the conditions that the xenon light spectrally filtered to the wavelength from 550 to 650 nm with an intensity of 0.32 W cm^{-2} was irradiated. b) The pH dependence of the H_2 (full circle and square) and O_2 (empty circle and square) evolution efficiency under the conditions that the pH value in the H_2 evolution side is fixed at 1 as plotted on red background and the pH value in the O_2 evolution side is fixed at 13 as plotted on blue background, respectively.

evolution side, and no production of H_2 or O_2 was observed at a pH value of 4. Therefore, a chemical bias was required in the water splitting in this system of at least 0.59 V, which corresponds to the difference between pH 3 and pH 13. However, a pH value of 1 was fixed on the H_2-evolution side, as indicated by the red background in Figure 3b, which is the condition that preferentially induces H_2 evolution. Similarly, the evolution efficiency of H_2 was twice that of O_2 at the observed pH value. In contrast, the evolution efficiency of both H_2 and O_2 gradually decreased with decreasing pH value on the O_2-evolution side. However, the evolution of both H_2 and O_2 was still observed, even at a pH of 6.8 using pure water. In addition, neither H_2 nor O_2 evolution was observed at a pH of 6. Therefore, in this system, a chemical bias was required in the water splitting of at least 0.34 V, which corresponds to the difference between pH 1 and pH 6.8. Therefore, the chemical bias required for the water splitting changes as the fixed pH value in the chamber changes.

To further explore the limiting pH conditions for H_2 and O_2 evolution, the pH values on the H_2- and O_2-evolution sides were fixed at 3 and 6.8, respectively, which are the minimum acidic and alkaline conditions observed in the previous experiments to promote evolution of H_2 and O_2, respectively. The irradiation time dependence of H_2 and O_2 evolution is shown in Figure 4a. The results confirm that the evolution of

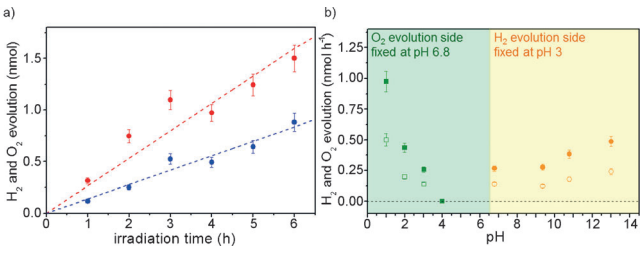

Figure 4. a) An irradiation time dependence of H_2 (red circle) and O_2 (blue circle) evolution at the pH combination of 3 and 6.8. b) The pH dependence of the H_2 (full circle and square) and O_2 (empty circle and square) evolution efficiency under the conditions that the pH value in the H_2 evolution side is fixed at 3 as plotted on yellow background and the pH value in the O_2 evolution side is fixed at 6.8 as plotted on green background, respectively.

both H_2 and O_2 increased approximately linearly with increasing irradiation time and that the efficiency of H_2 evolution was twice that of O_2 evolution. The pH dependence is shown in Figure 4b, which is summarized as being analogous to Figure 3b. The evolution efficiency of both H_2 and O_2 gradually decreased with increasing pH on the H_2-evolution side, and no production of H_2 or O_2 was observed at pH 4. When the pH value was set to 4 on the H_2-evolution side, the water splitting did not proceed at either pH value on the O_2-evolution side. This result indicates that the reaction rate of hydrogen evolution is the rate-determining process in water splitting. In addition, the absolute efficiency is significantly lower than the previous data because of the insufficient chemical bias applied to that system. In the case where the pH value on the H_2-evolution side was fixed, water splitting was induced, even at a pH combination of 3 and 6.8, which corresponds to a minimum chemical bias of 0.23 V in this plasmon-assisted water splitting system.[11] As far as we know, this chemical bias is the smallest value reported for a water splitting system driven by visible-light irradiation.

The pH dependence experiments clearly demonstrated that the pH dependence of water splitting exhibits an asymmetrical response. The mechanism for water oxidation is considered to rely on the adsorption of OH^- onto the surface of $SrTiO_3$, close to the Au-NPs. In addition, the efficiency of O_2 evolution is strongly dependent on the concentration of OH^-, as defined by the pH value, because the adsorbed hydroxyl ions must be oxidized by multiple electron holes to evolve oxygen.[12] However, under neutral conditions, such as pH 6.8, the surface concentration of OH^- is lower than that under alkaline conditions. Water molecules must dissociate to form adsorbed OH^- on the surface of $SrTiO_3$, thereby resulting in the observation that the reaction rate of water oxidation is lower than that of OH^- oxidation. Notably, the effective water-splitting process proceeds under neutral conditions in the present system, which suggests that water molecules could be directly oxidized by the plasmon-induced water splitting system. Thus, the efficient oxidation of water and OH^- also requires highly concentrated electron holes at a local site because multiple electron-transfer processes are required with two water molecules or four OH^- groups. The possibility exists that the LSPR generates multiple holes at the plasmonically enhanced optical near-field because of an efficient charge separation and that the multiple holes trapped at the surface states of $SrTiO_3$ near the hot site might be stored at a local site of the $SrTiO_3$. The stored multiple holes confined at a local site of the $SrTiO_3$ may be able to accelerate the oxidation of water or OH^- and the subsequent evolution of oxygen.

Figure 5 illustrates the energy diagram of the plasmon-induced water splitting system based on the Au-NP-loaded $SrTiO_3$ photoelectrode at the pH combination of 3 and 6.8. We hypothesized that an excited electron is transferred into the conduction band of $SrTiO_3$ immediately following the inter- or intraband transition of the Au-NPs induced by the plasmonically enhanced optical near-field or by hot electron transfer, thus leaving an electron hole trapped at the surface state of the $SrTiO_3$ near the Au/$SrTiO_3$/water interface. The trapped holes can subsequently induce efficient oxidation of

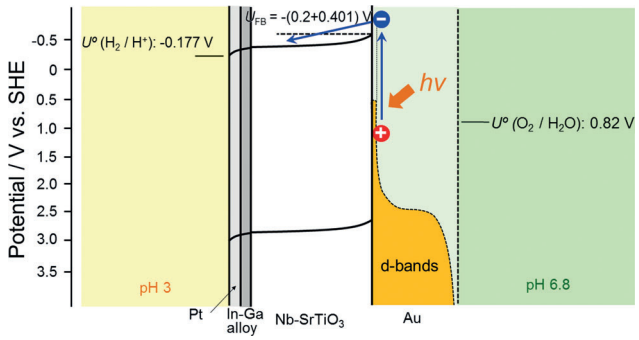

Figure 5. Energy diagram of the plasmon-induced water splitting system using Au-NPs loaded $SrTiO_3$ substrate at the pH combination of 3 and 6.8. The flat band potential of $SrTiO_3$ at pH 6.8 was estimated as −0.601 V vs. standard hydrogen electrode (SHE) because the potential of the conduction band of $SrTiO_3$ is known to be −0.2 V vs. SHE at pH 0. The difference in the potential of 0.401 V is due to pH difference.

hydroxyl ions by multi-electron transfer.[13] However, the photogenerated electrons injected into the conduction band of $SrTiO_3$ induce the reduction of a proton at the Pt surface to adhere to the backside of the $SrTiO_3$ photoelectrode. Thus, plasmon-induced water splitting was clearly demonstrated, and the efficient water oxidation due to the plasmon effect reduced the chemical bias by 0.23 V.

In conclusion, we successfully developed a simple plasmon-induced water splitting system without an external electrochemical apparatus by using two sides of the same $SrTiO_3$ single-crystal substrate. The huge advantage using plasmonic Au nanostructures is stable over time unlike molecular sensitizers and its resonant wavelength can be tuned by simply changing their shape and/or size to cover a large part of the solar spectrum. Actually, we confirmed the stability of the plasmon-assisted water splitting system with a longer time irradiation. The linear relationship of both H_2 and O_2 evolution was obviously observed even with an irradiation of 48 h as described in the Supporting Information. A stoichiometric evolution of H_2 and O_2 was simultaneously obtained from two separate solution chambers. The separate evolution of H_2 and O_2 is expected to suppress the recombination of the two gases. Even the irradiation of the unprecedented long wavelength from 750 to 850 nm succeeded in water splitting. The mechanism for the water splitting device occurs through plasmon-induced charge separation at the Au-NP/$SrTiO_3$ interface, thereby promoting water oxidation and subsequent reduction of a proton on the backside of the $SrTiO_3$ substrate. The pH dependence experiments revealed that the chemical bias is substantially reduced by plasmonic effects up to 0.23 V because of efficient water oxidation. Although the apparent quantum efficiency is still low (4.4×10^{-4}% at 600 nm), these results indicate the possibility of constructing an efficient artificial photosynthesis system that responds to visible and near-infrared light and does not need the chemical bias through the combination of an efficient co-catalyst for H_2 evolution on the backside of a $SrTiO_3$ substrate as well as understanding the detailed mechanism.

Experimental Section

Preparation of Au-NPs on a $SrTiO_3$ substrate: Single-crystal strontium titanate ($SrTiO_3$, 0.05 wt% niobium doped, $10\times10\times0.5$ mm^3, Furuuchi Chemical) with a (110) surface was used as a semiconductor substrate for water splitting. The $SrTiO_3$ substrate was rinsed with acetone, methanol, and deionized water in an ultrasonic bath for 5 min and was dried under a flow of pure nitrogen. A thin gold film (3 nm) was deposited onto the front side of the $SrTiO_3$ by helicon sputtering (MPS-4000, ULVAC) at a deposition rate of 1 Å s^{-1} and was annealed at a temperature of 800 °C for 1 h in a nitrogen atmosphere to load the Au-NPs onto the $SrTiO_3$ surface.[14] The Au-NPs on the $SrTiO_3$ surface were observed by field-emission scanning electron microscopy (FE-SEM, JSM-6700FT, JEOL). The maximum resolution attainable at an electron acceleration voltage of 15 kV was 1 nm.

Construction of the water splitting device: An In-Ga alloy (4:1 weight ratio) paste was applied to the backside of the $SrTiO_3$ substrate to form Ohmic contacts. Subsequently, a Pt board ($10\times10\times0.5$ mm^3, 99.98%, Nilaco Corporation) was adhered to the backside of the substrate by the Ag paste (D-550, Fujikura Kasei). The water splitting device contained sealed reaction cells with two solution compartments separated by the $SrTiO_3$ substrate. The Au-NP-loaded surface was on the front side of the photoelectrode, which was irradiated by visible light to induce O_2 evolution, whereas a Pt board was used for H_2 evolution on the backside. To adjust the chemical bias between the H_2- and O_2-evolution chambers, the pH was regulated using arbitrary concentrations of hydrochloric acid (HCl) and potassium hydroxide (KOH) aqueous solutions. The volume of H_2- and O_2-evolution chambers are 600 and 230 μL, respectively. To maintain the charge balance between the chambers, a salt bridge with 2 wt% agar was used. The pH values of the solutions were examined using a pH meter (AS600, AS ONE).

Received: May 2, 2014
Published online: July 2, 2014

Keywords: electrochemistry · localized surface plasmons · nanostructures · photochemistry · water splitting

[1] a) D. Gust, T. A. Moore, A. L. Moore, *Acc. Chem. Res.* **2001**, *34*, 40–48; b) N. S. Lewis, D. G. Nocera, *Proc. Natl. Acad. Sci. USA* **2006**, *103*, 15729–15735; c) P. V. Kamat, *J. Phys. Chem. C* **2007**, *111*, 2834–2860; d) S. Linic, P. Christopher, D. B. Ingram, *Nat. Mater.* **2011**, *10*, 911–921.

[2] a) A. Fujishima, K. Honda, *Bull. Chem. Soc. Jpn.* **1971**, *44*, 1148–1150; b) A. Fujishima, K. Honda, *Nature* **1972**, *238*, 37–38.

[3] a) M. Graetzel, *Acc. Chem. Res.* **1981**, *14*, 376–384; b) N. Vlachopoulos, P. Liska, J. Augustynski, M. Graetzel, *J. Am. Chem. Soc.* **1988**, *110*, 1216–1220; c) H. Rensmo, K. Keis, H. Lindström, S. Södergren, A. Solbrand, A. Hagfeldt, S. E. Lindquist, L. N. Wang, M. Muhammed, *J. Phys. Chem. B* **1997**, *101*, 2598–2601; d) Y. Nishijima, K. Ueno, Y. Yokota, K. Murakoshi, H. Misawa, *J. Phys. Chem. Lett.* **2010**, *1*, 2031–2036; e) Y. Nishijima, K. Ueno, Y. Kotake, K. Murakoshi, H. Inoue, H. Misawa, *J. Phys. Chem. Lett.* **2012**, *3*, 1248–1252.

[4] a) G. Liu, L. Wang, H. G. Yang, H.-M. Cheng, G. Q. Lu, *J. Mater. Chem.* **2010**, *20*, 831–843; b) A. Kudo, H. Kato, I. Tsuji, *Chem. Lett.* **2004**, *33*, 1534–1539; c) H. Tada, T. Mitsui, T. Kiyonaga, T. Akita, K. Tanaka, *Nat. Mater.* **2006**, *5*, 782–786; d) H. Kato, M. Hori, R. Konta, Y. Shimodaira, A. Kudo, *Chem. Lett.* **2004**, *33*, 1348–1349; e) K. Sayama, K. Mukasa, R. Abe, Y. Abe, H. Arakawa, *J. Photochem. Photobiol. A* **2002**, *148*, 71–77.

[5] a) J. H. Park, S. Kim, A. J. Bard, *Nano Lett.* **2006**, *6*, 24–28; b) R. Asahi, T. Morikawa, T. Ohwaki, K. Aoki, Y. Taga, *Science* **2001**, *293*, 269–271; c) H. Irie, Y. Watanabe, K. Hashimoto, *Chem.*

Lett. **2003**, *32*, 772 – 773; d) Q. Li, Y. W. Li, P. Wu, R. Xie, J. K. Shang, *Adv. Mater.* **2008**, *20*, 3717 – 3723; e) T. Ohno, T. Mitsui, M. Matsumura, *Chem. Lett.* **2003**, *32*, 364 – 365; f) X. Chen, C. Burda, *J. Am. Chem. Soc.* **2008**, *130*, 5018 – 5019; g) T. Umebayashi, T. Yamaki, H. Itoh, K. Asai, *J. Phys. Chem. Solids* **2002**, *63*, 1909 – 1920; h) K. Zakrzewska, M. Radecka, M. Rekas, *Thin Solid Films* **1997**, *310*, 161 – 166.

[6] a) K. Maeda, T. Takata, M. Hara, N. Saito, Y. Inoue, H. Kobayashi, K. Domen, *J. Am. Chem. Soc.* **2005**, *127*, 8286 – 8287; b) K. Maeda, K. Teramura, D. Lu, N. Saito, Y. Inoue, K. Domen, *J. Phys. Chem. C* **2007**, *111*, 7554 – 7560; c) K. Maeda, K. Domen, *J. Phys. Chem. C* **2007**, *111*, 7851 – 7861; d) W. J. Youngblood, S.-H. A. Lee, Y. Kobayashi, E. A. Hernandez-Pagan, P. G. Hoertz, T. A. Moore, A. L. Moore, D. Gust, T. E. Mallouk, *J. Am. Chem. Soc.* **2009**, *131*, 926 – 927; e) W. J. Youngblood, S.-H. A. Lee, K. Maeda, T. E. Mallouk, *Acc. Chem. Res.* **2009**, *42*, 1966 – 1973; f) Y. H. Ng, A. Iwase, A. Kudo, R. Amal, *J. Phys. Chem. Lett.* **2010**, *1*, 2607 – 2612; g) M. Higashi, K. Domen, R. Abe, *J. Am. Chem. Soc.* **2013**, *135*, 10238 – 10241.

[7] a) A. Ishikawa, T. Takata, J. N. Kondo, M. Hara, H. Kobayashi, K. Domen, *J. Am. Chem. Soc.* **2002**, *124*, 13547 – 13553; b) A. Kudo, K. Omori, H. Kato, *J. Am. Chem. Soc.* **1999**, *121*, 11459 – 11467.

[8] a) C. Perkins, A. W. Weimer, *Int. J. Hydrogen Energy* **2004**, *29*, 1587 – 1599; b) L. J. Minggu, W. R. W. Daud, M. B. Kassim, *Int. J. Hydrogen Energy* **2010**, *35*, 5233 – 5244; c) K. Maeda, K. Domen, *J. Phys. Chem. Lett.* **2010**, *1*, 2655 – 2661.

[9] a) E. Selli, G. L. Chiarello, E. Quartarone, P. Mustarelli, I. Rossetti, L. Forni, *Chem. Commun.* **2007**, 5022 – 5024; b) M. Kitano, M. Takeuchi, M. Matsuoka, J. A. Thomas, M. Anpo, *Catal. Today* **2007**, *120*, 133 – 138.

[10] W.-N. Wang, W.-J. An, B. Ramalingam, S. Mukherjee, D. M. Niedzwiedzki, S. Gangopadhyay, P. Biswas, *J. Am. Chem. Soc.* **2012**, *134*, 11276 – 11281.

[11] a) C. Gomes Silva, R. Juarez, T. Marino, R. Molinari, H. Garcia, *J. Am. Chem. Soc.* **2011**, *133*, 595 – 602; b) E. Thimsen, F. Le Formal, M. Grätzel, S. C. Warren, *Nano Lett.* **2011**, *11*, 35 – 43; c) J.-J. Chen, J. C. S. Wu, P. C. Wu, D. P. Tsai, *J. Phys. Chem. C* **2011**, *115*, 210 – 216; d) D. B. Ingram, S. Linic, *J. Am. Chem. Soc.* **2011**, *133*, 5202 – 5205; e) H. M. Chen, C. K. Chen, C.-J. Chen, L.-C. Cheng, P. C. Wu, B. H. Cheng, Y. Z. Ho, M. L. Tseng, Y.-Y. Hsu, T.-S. Chan, J.-F. Lee, R.-S. Liu, D. P. Tsai, *ACS Nano* **2012**, *6*, 7362 – 7372; f) S. C. Warren, E. Thimsen, *Energy Environ. Sci.* **2012**, *5*, 5133 – 5146.

[12] O. Diaz-Morales, F. Calle-Vallejo, C. de Munck, M. T. M. Koper, *Chem. Sci.* **2013**, *4*, 2334 – 2343.

[13] a) S. Pillai, K. R. Catchpole, T. Trupke, M. A. Green, *J. Appl. Phys.* **2007**, *101*, 093105; b) Z. Liu, W. Hou, P. Pavaskar, M. Aykol, S. B. Cronin, *Nano Lett.* **2011**, *11*, 1111 – 1116; c) I. Thomann, B. A. Pinaud, Z. Chen, B. M. Clemens, T. F. Jaramillo, M. L. Brongersma, *Nano Lett.* **2011**, *11*, 3440 – 3446.

[14] X. Shi, K. Ueno, N. Takabayashi, H. Misawa, *J. Phys. Chem. C* **2013**, *117*, 2494 – 2499.

